Journal of The Electrochemical Society, **160** (3) A444-A448 (2013)
0013-4651/2013/160(3)/A444/5/$28.00 © The Electrochemical Society

Factors that Affect the Phase Behavior of Multi-Component Olivine ($LiFe_xMn_yCo_{1-x-y}PO_4$; $0 < x, y < 1$) in Lithium Rechargeable Batteries: One-Phase Reaction vs. Two-Phase Reaction

Kyu-Young Park,[a] Jihyun Hong,[a] Jongsoon Kim,[a] Young-Uk Park,[a] Haegyeom Kim,[a] Dong-Hwa Seo,[a] Sung-Wook Kim,[a] Jang-Wook Choi,[b,*] and Kisuk Kang[a,c,z]

[a]*Department of Materials Science and Engineering, Seoul National University, Gwanak-gu, Seoul 151-742, Korea*
[b]*Graduate School of EEWS, KAIST, Yuseong-gu, Daejeon 305-701, Korea*
[c]*Department of Materials Science and Engineering, Research Institute of Advanced Materials, Seoul National University, Seoul, 151-742, Republic of Korea*

The structural evolution of multi-component olivines upon delithiation and lithiation was investigated by ex-situ X-ray diffraction. We found that one-phase de/lithiation occurs for multi-component olivines for a fairly large compositional range of transition metal species given that two-phase de/lithiation is generally accepted for olivine cathodes. We discuss the driving force that determines the phase behavior (two-phase reaction vs. one-phase reaction) of olivines in terms of enthalpy of mixing presumably dominated from the electrostatic interaction among cations and the elastic strain stored in the crystal due to the volume change of redox active element. We believe that this fundamental study on the phase behavior of olivines will provide insight into the intrinsic electrochemical properties of olivine electrodes for rechargeable lithium batteries.
 [DOI: 10.1149/2.036303jes]

Manuscript submitted May 7, 2012; revised manuscript received December 17, 2012. Published January 4, 2013.

$LiMPO_4$ olivine electrodes (M = Mn, Fe, Co, Ni) in Li batteries store and release Li ions through a two-phase reaction between the Li-rich $Li_{1-x}MPO_4$ and the Li-deficient Li_xMPO_4 ($x \sim 0$).[1–16] However, a one-phase reaction of the olivine structure during charging/discharging has been recently reported.[12,15,17–20]Gibot et al. and Delacourt et al. demonstrated that conversion from a two-phase to one-phase reaction can occur for $LiFePO_4$ olivine that contains significant amount of disorder among Li and Fe or at an elevated temperature[15,17] and Cogswell et al. reported that size and temperature dependent-solubility in $LiFePO_4$ can be explained by coherency strain in crystal structure by a regular solution model.[21] Yamada et al. also reported that the binary olivines $LiMn_xFe_{1-x}PO_4$ can operate *via* a partially one-phase reaction for a certain range of lithium content.[19] Furthermore, Gwon et al. showed that the ternary olivine $LiMn_{1/3}Fe_{1/3}Co_{1/3}PO_4$ can operate *via* a fully one-phase reaction during charging/discharging.[18] Since electrochemical properties are strongly dependent on the phase behavior of the electrode, a change in phase reaction can substantially affect the electrochemical performance.

The theoretical efforts to understand this unique phenomenon of the olivine have been made by a few groups. It was claimed that the dominant factor determining the phase behavior of the Li_xFePO_4 olivines are positive enthalpy mixing derived from the enthalpy of mixing presumably dominated from the electrostatic interaction between cations or vacancies by Zhou et al.[3,22] While Li^+–Li^+ or vacancy–vacancy interactions disfavor two-phase segregation, the effective attraction between Li^+–Fe^{2+} or vacancy–Fe^{3+} favors two-phase behavior. Cogswell et al. demonstrated using phase-field modeling that one-phase behavior of $LiFePO_4$ can be promoted in the presence of coherency strain in crystal structure by a regular solution model.[21] Also, our recent work on the multi-component $LiFe_{1/3}Mn_{1/3}Co_{1/3}PO_4$ olivine, in the context of enthalpy of mixing dominated from the electrostatic interaction, suggested the one-phase reaction based battery operation of multi-component olivine because of the different redox potentials of Fe, Mn and Co and their random distribution in the structure, which weakens the effective attraction between Li^+-M^{2+} (M = Fe, Mn, Co). In this work, however, we found that depending on the composition of transition metal species in the olivine, the phase behavior is sensitively affected between one-phase reaction and two-phase reaction.

A series of $LiFe_xMn_yCo_{1-x-y}PO_4$ ($0 < x, y < 1$) samples were prepared and their structural evolution was investigated as a function of lithium content using ex-situ structural analysis. One-phase characteristic of multi-component olivine is significantly weakened, in particular, for Mn-rich multi-component olivines which we attribute to the larger degree of volume change of Mn ions during redox reaction in the structure.

Experimental

Preparation of multi-component olivines.— $LiFe_xMn_yCo_{1-x-y}PO_4$ ($0 < x, y < 1$) samples were synthesized using a solid-state method using co-precipitated metal oxalate sources ($(Fe_xMn_yCo_{1-x-y}) \cdot 2H_2O$ ($0 < x, y < 1$)).[23] A stoichiometric amount of $MnSO_4 \cdot H_2O$ (99%, Aldrich), $(NH_4)_2Fe(SO_4)_2 \cdot 7H_2O$ (99%, Aldrich), $CoSO_4 \cdot 7H_2O$ (99%, Aldrich), and $(NH_4)_2C_2O_4 \cdot H_2O$ (99%, Aldrich) were used as precursors (Supporting Table 1s).[41] Initially, 0.7 M aqueous solutions of ammonium oxalate and 0.5 M of mixed metals were prepared. The metals solution was added dropwise to the oxalate solution with stirring. The co-precipitation was continued in an Ar-filled glove box for 6 hr at 90°C. The precipitate was isolated by filtration, washed with de-ionized water, and then dried at 120°C for 2 hours.

Multi-component olivines having various compositions were synthesized by a solid-state reaction using the prepared oxalate source, LiH_2PO_4 (98%, Aldrich), and pyromellitic acid hydrate (6 wt%, PA, 99%, Fluka) as the organic additive. The mixtures were ball-milled in acetone for 18 hr. After drying at 70°C, the mixtures were fired at 500°C under Ar for 10 hr. For carbon coating, 6 wt% of pyromellitic acid hydrate, 1 wt% of ferrocene (98%, Aldrich), and 93 wt% of the calcined mixture were ball-milled with acetone for 2 hr. After evaporation of the acetone at 70°C, the dried mixture was pelletized under 200 kg cm^{-2} pressure for 10 s in a disk-shaped mold. The pelletized mixture was fired again at 600°C under Ar for 10 hr.

Electrochemical Characterization

For the electrochemical characterization, we dispersed 79 wt% active material, 12 wt% carbon black, and 9 wt% polyvinylidene fluoride (PVDF) in N-methyl-2-pyrrolidone (NMP). The prepared slurry was cast on aluminum foil and dried at 120°C for 2 hours. Electrochemical cells were assembled using a CR2016 coin cell with lithium metal as a counter electrode, a separator (Celgard 2400), and 1 M $LiPF_6$ electrolyte in ethyl carbonate/dimethyl carbonate (Techno Semichem, EC/DMC, 1:1 v/v) in an Ar-filled glove box. The electrochemical performance was tested at 2.5–4.8 V at C/10 at room temperature using a potentio-galvanostat.

Ex-situ XRD.— To investigate the structural evolution of Li_xMPO_4 ($x = 0 - 1$) during the electrochemical reaction, ex-situ X-ray diffraction (XRD) patterns of the test electrodes were collected as a function

*Electrochemical Society Active Member.
zE-mail: matlgen1@snu.ac.kr

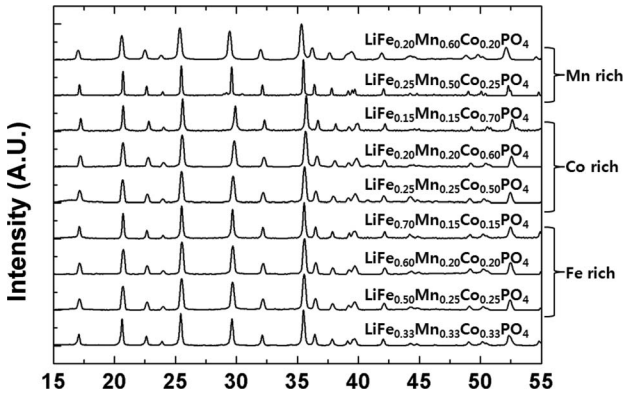

Figure 1. XRD patterns of multi-component olivines. The XRD patterns are good matches to the typical olivine XRD pattern. No noticeable impurities are evident.

of the charge state at the rate of C/10. The electrochemical cell was disassembled in an Ar-filled glove box. Electrodes were washed with DMC to remove residual $LiPF_6$ salt. After drying the electrodes for 20 min, diffraction patterns of the electrodes were recorded. The XRD measurements were performed using Cu–Kα radiation with a step size of 0.02° in the 2θ range of 15–55°.

Results and Discussion

Preparation of multi-component olivines.— We prepared a series of multi-component olivines ($LiFe_xMn_yCo_{1-x-y}PO_4$, $0 < x, y < 1$)

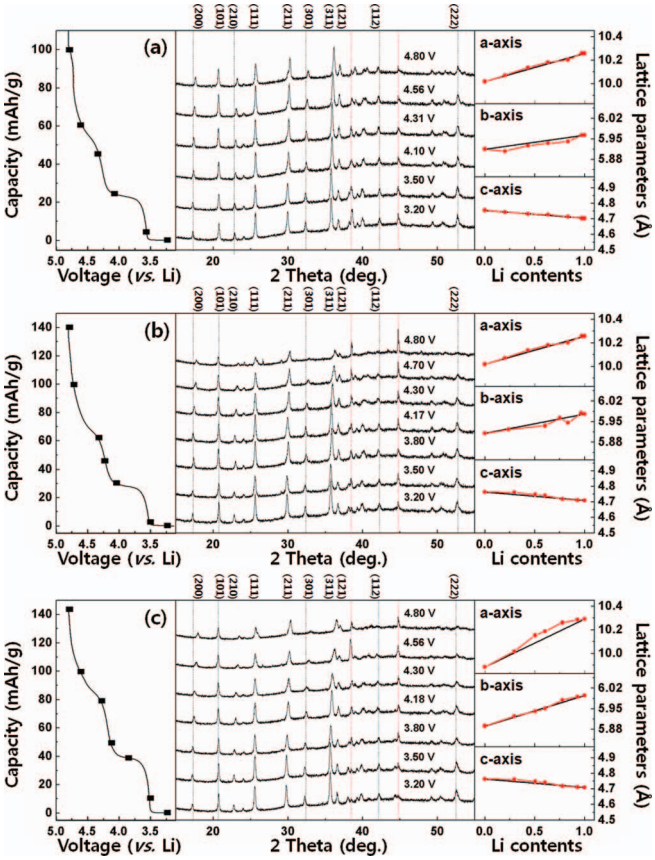

Figure 2. Ex-situ XRD patterns(midle), first charge curve(left) and lattice parameters change as a function of lithium contents(right) at sample (a) $LiFe_{0.15}Mn_{0.15}Co_{0.70}PO_4$, (b) $LiFe_{0.20}Mn_{0.20}Co_{0.60}PO_4$and (c) $LiFe_{0.25}Mn_{0.25}Co_{0.50}PO_4$. The red line in the XRD patterns is the Al peak position.

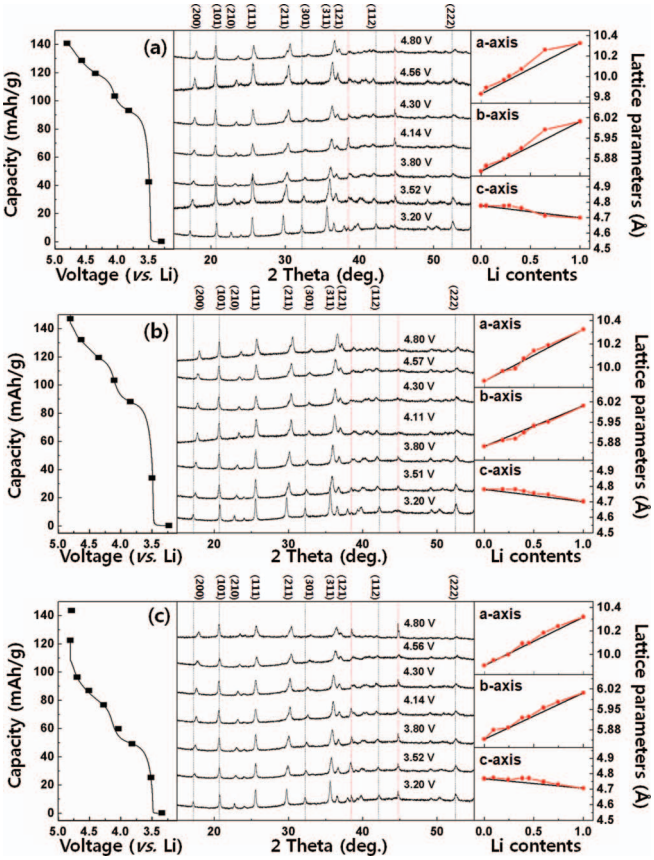

Figure 3. Ex-situ XRD patterns(midle), first charge curve(left) and lattice parameters change as a function of lithium contents (right) at sample (a) $LiFe_{0.70}Mn_{0.15}Co_{0.15}PO_4$, (b) $LiFe_{0.60}Mn_{0.20}Co_{0.20}PO_4$ and (c) $LiFe_{0.50}Mn_{0.25}Co_{0.25}PO_4$. The red line in the XRD patterns is the Al peak position.

with different compositions: Mn-rich: $LiFe_{0.20}Mn_{0.60}Co_{0.20}PO_4$, and $LiFe_{0.25}Mn_{0.50}Co_{0.25}PO_4$; Fe–rich: $LiFe_{0.70}Mn_{0.15}Co_{0.15}PO_4$, $LiFe_{0.60}Mn_{0.20}Co_{0.20}PO_4$, and $LiFe_{0.50}Mn_{0.25}Co_{0.25}PO_4$; and Co–rich: $LiFe_{0.15}Mn_{0.15}Co_{0.70}PO_4$, $LiFe_{0.20}Mn_{0.20}Co_{0.60}PO_4$, and $LiFe_{0.25}Mn_{0.25}Co_{0.50}PO_4$. The morphologies of the samples are shown in Supporting Figure 1s.[41] The particle sizes of all samples were comparable at about 200 nm. The phase purity of pristine samples was identified by XRD analysis (Figure 1). XRD patterns matched the *Pnma* space group of the general olivine crystal well with no noticeable impurities. Structural refinement was performed for the *Pnma* space group with Li in the 4a position and transition metals in the 4c position for all samples. The refined lattice parameters are tabulated in Supporting Table 2s.[41] The measured lattice parameters agreed well (within 0.05%) with those expected from Vegard's law based on the Fe :Mn : Co composition. Mn-rich olivines tended to have larger lattice parameters than Fe–rich and Co-rich olivines because of the slightly larger ionic size of Mn^{2+} (> Fe^{2+} > Co^{2+}).[24] This indicated that a solid solution of $LiFePO_4$, $LiMnPO_4$, and $LiCoPO_4$ had formed without segregation of the individual $LiMPO_4$ (M = Mn, Fe, Co) phases.

Phase behavior of multi-component olivines during an electrochemical reaction.— We investigated the structural evolution of multi-component olivine electrodes as a function of Li content using ex-situ XRD analysis. While the phase behavior from the ex-situ measurement may differ from what is really happening in-situ measurement due to kinetic factors,[25] the ex-situ analysis is an effective tool to observe the equilibrium state at zero current. The measurements were taken during the first charge at the C/10 rate (Figures 2–4). All electrochemical profiles exhibited three

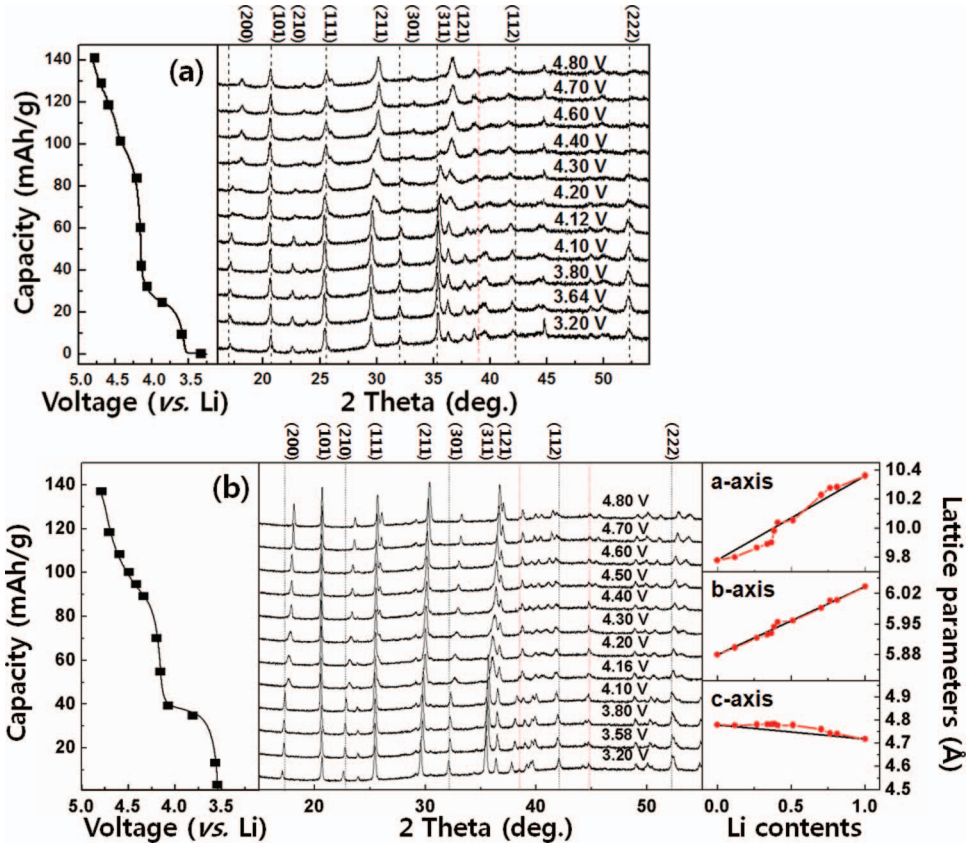

Figure 4. Ex-situ XRD patterns(midle), first charge curve(left) and lattice parameters change as a function of lithium contents at sample (a) $LiFe_{0.25}Mn_{0.60}Co_{0.25}PO_4$ sample and (b) $LiFe_{0.20}Mn_{0.50}Co_{0.20}PO_4$. The red line in the XRD patterns is the Al peak position.

distinctive pseudo-plateau attributable to Fe^{2+}/Fe^{3+}, Mn^{2+}/Mn^{3+}, and Co^{2+}/Co^{3+} redox couples.[12,19,26,27] The length of a pseudo-plateau depends on the ratio of the transition metals in the olivine. Our previous study showed that one-phase-based delithiation/lithiation occurred for $LiFe_{1/3}Mn_{1/3}Co_{1/3}PO_4$ upon electrochemical cycling.[18] Similar behavior was observed for Co-rich and Fe-rich olivines (Figures 2 and 3). For these compositional olivines, all diffraction peaks steadily shifted throughout the whole delithiation procedure; no new peaks appeared. The refined lattice parameters for the partially delithiated samples were in good agreement with the expected weight-averaged lattice parameters for $x\text{LiMPO}_4$ and $(1-x)\text{MPO}_4$. This indicates that the Co-rich and Fe-rich multi-component olivines operate *via* a one-phase reaction upon electrochemical cycling. This one-phase reaction occurred at a fairly broad compositional range of Fe and Co, that is, up to 70% of Fe or Co. We and others[23] have previously explained this unusual (relative to single-component olivines) one-phase delithiation behavior of the multi-component olivines on the basis of effective enthalpy of mixing presumably dominated from the electrostatic interaction between ions within the olivine crystal. When strong charge localization occurs in an olivine crystal because of the relatively long transition metal−transition metal distance, the driving force for the two-phase behavior or phase-separation of the olivine during delithiation could be understood in terms of two competing energy terms. One force is based on the repulsive interactions between Li^+-Li^+ (or vacancy(V)–vacancy) and between $M^{3+}-M^{3+}$ (or $M^{2+}-M^{2+}$), which are present when $Li^+M^{2+}PO_4$ and $VM^{3+}PO_4$ coexist.[3,12,18,23] This repulsive term inhibits phase separation. On the other hand, attractive interactions between Li^+-M^{2+} and between $V-M^{3+}$ are present within the crystal, favoring phase separation. In general, the latter prevails for simple olivines, resulting in a two-phase reaction.[3] However, in the case of multi-component olivines, Li^+ ions are often surrounded simultaneously by M^{2+} and M^{3+} ions during de/lithiation. This is because the different transition metal ions are uniformly distributed and have quite different redox potentials.[12] This weakens the latter force by reducing the number of Li^+-M^{2+} attractive interaction, which leads to a one-phase reaction.

A partial two-phase reaction was, on the contrary, observed for Mn-rich olivines at a relatively lower concentration of major element, Mn. While a full one-phase reaction was observed at a Mn composition as high as 50% ($LiFe_{0.25}Mn_{0.50}Co_{0.25}PO_4$), evidence of two-phase behavior emerged when the Mn content reached 60% ($LiFe_{0.20}Mn_{0.60}Co_{0.20}PO_4$). Figure 4a clearly shows that a new delithiated phase emerged above 4 V before becoming a solid solution again. This is contrast to Co-rich or Fe-rich multi-component olivines which showed full one-phase reaction even at 70% of the major element (Fe for Fe-rich $LiMn_{0.15}Fe_{0.70}Co_{0.15}PO_4$ and Co for Co-rich $LiMn_{0.15}Fe_{0.15}Co_{0.70}PO_4$) in compositions (Figure 2a, 3a). This partial two-phase reaction in Mn-rich multi-component olivines strongly implies that factors other than enthalpy of mixing dominated from the electrostatic interaction affect on the phase behavior. Let us consider that half of the Li ions are extracted from $LiMPO_4$ by a one-phase reaction. In this case, half of the M^{2+} are oxidized to M^{3+}, so there will be both electrostatic repulsion and attraction among Li^+-M^{3+} and Li^+-M^{2+} in the crystal. For instance, Li ions in Mn-rich $Li_{0.5}Mn_{0.60}Fe_{0.20}Co_{0.20}PO_4$ will have a 1:1 ratio of M^{2+} ($0.3Mn^{2+}$ and $0.2Co^{2+}$) and M^{3+} ($0.2Fe^{3+}$ and $0.3Mn^{3+}$) as neighbors, which will provide attractive and repulsive interactions affecting the phase behavior. A similar force balance will occur for Fe-rich $Li_{0.5}Mn_{0.2}Fe_{0.60}Co_{0.20}PO_4$ with a 1:1 ratio of M^{2+} ($0.2Mn^{2+}$, $0.1Fe^{2+}$, and $0.2Co^{2+}$) and M^{3+} ($0.5Fe^{3+}$) as Li ion neighbors. Considering electrostatic terms only, these two materials should show the same phase behavior. But in fact, the $Li_{0.5}Mn_{0.60}Fe_{0.20}Co_{0.20}PO_4$ is susceptible to phase separation into lithium-rich and lithium–poor phases, while $Li_{0.5}Mn_{0.20}Fe_{20}PO_4$ is stable as a single phase. The reason for this discrepancy is discussed in the following section.

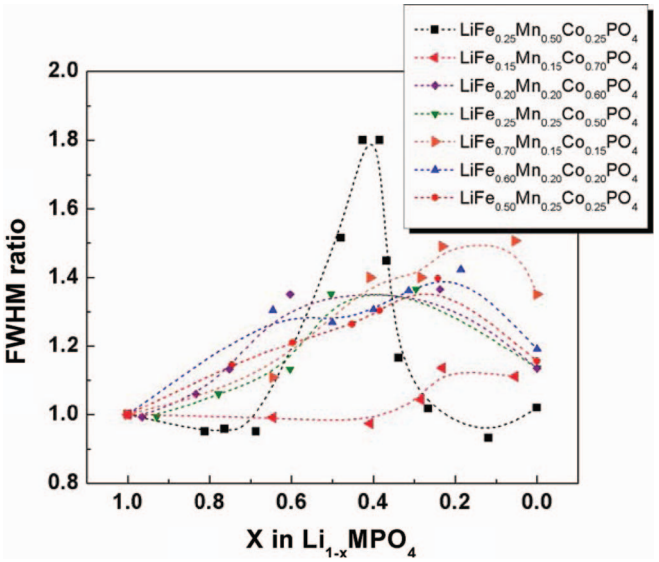

Figure 5. FWHM ratios for the (200) peak. The ratio is based on FWHM (Li_xMPO_4) / FWHM ($LiMPO_4$).

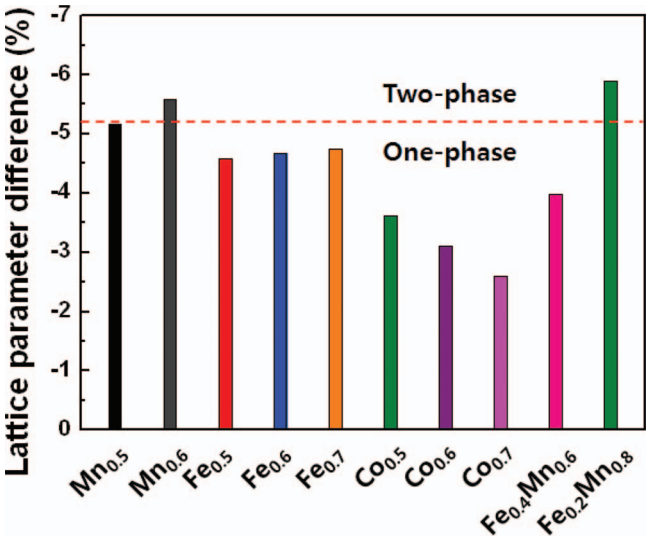

Figure 6. *a*-axis lattice parameter difference. $(a_{Li\text{-}rich} - a_{Li\text{-}poor})/a_{Li\text{-}rich}$. $Mn_{0.5}$ = $LiFe_{0.25}Mn_{0.50}Co_{0.25}PO_4$, $Mn_{0.6}$ = $LiFe_{0.20}Mn_{0.60}Co_{0.20}PO_4$, $Fe_{0.5}$ = $LiFe_{0.50}Mn_{0.25}Co_{0.25}PO_4$, $Fe_{0.6}$ = $LiFe_{0.60}Mn_{0.20}Co_{0.20}PO_4$, $Fe_{0.7}$ = $LiFe_{0.70}Mn_{0.15}Co_{0.15}PO_4$, $Co_{0.5}$ = $LiFe_{0.25}Mn_{0.25}Co_{0.50}PO_4$, $Co_{0.6}$ = $LiFe_{0.20}Mn_{0.20}Co_{0.60}PO_4$, $Co_{0.7}$ = $LiFe_{0.15}Mn_{0.15}Co_{0.70}PO_4$, $Fe_{0.4}Mn_{0.6}$ = $LiFe_{0.4}Mn_{0.6}PO_4$, $Fe_{0.2}Mn_{0.8}$ = $LiFe_{0.2}Mn_{0.8}PO_4$. $Fe_{0.4}Mn_{0.6}$ and $Fe_{0.2}Mn_{0.8}$ data are taken from Reference 19.

Internal lattice strain and structural evolution.— Close examination of the XRD patterns of samples exhibiting one-phase reaction behavior shows that the degree of peak broadening is dependent on the transition metal compositions and lithium contents. Considering that particle size is unchanged during the charging process, the peak broadening primarily derives from the heterogeneous distortion in their crystal structures.[28] Figure 5 summarizes the Li contents and full-width at half-maximum (FWHM) data for the (200) peak for all samples. While the FWHM generally increased in the partially delithiated states, dramatic increase was exhibited in Mn-rich $LiMn_{0.50}Fe_{0.25}Co_{0.25}PO_4$. It was noted that higher Mn-content sample does not exhibit one-phase behavior and precipitate the second phase. This observation coincides with the fact that the volume change (or lattice misfit) of two phases in $LiMnPO_4$-based olivine is the largest among olivines that undergo two-phase reaction. These effects are attributable to the Jahn–Teller effect of Mn^{+3}.[29,30] It leads us to consider the relationship between the tendency for phase separation and the lattice strain.

According to the general alloy theory, the coherent strain increases the energy of both phase and eventually promotes the formation of solid-solution rather than phase separation.[31] It was also demonstrated for $LiFePO_4$ with varying lithium solubility depending on particle size and temperature by phase field calculations.[21] The coherent strain occurred to minimize strain energy in the crystal structure,[21,32–35] and, as a result, strongly suppressed a phase separation between Li-rich phase and Li-poor phase.[21] Considering coherency strain in crystal structure, Mn-rich multi-component olivine has to show large solid-solution region because of the large volumetric change during delithiation. However, the Mn-rich samples show higher tendency for phase separation, and this observation is consistent with the finding for binary $LiFe_xMn_yPO_4$ ($x + y = 1$), which also displays a higher tendency toward a two-phase reaction for Mn-rich cases with $y > 0.5$.[19] In this respect, we believed that there exists critical lattice misfit for storing coherent strain in the olivine framework.

The elastic strain energy from coherent strain between similar crystal structures increases the Gibbs free energy of both crystals and promotes a solid-solution behavior. However, in general, the interface cannot stay in coherency above 5% lattice misfit. With higher than 5% misfit, it makes incoherent phase separation to reduce coherency strain energy.[37] Similarly, we expect that the multi-component olivine also has critical lattice misfit for coherent strain in the crystal structure. In this respect, among *a*, *b* and *c* lattice parameters, we particularly focused on the *a* lattice misfit, which is expected to strongly affect on the phase behavior due to the following aspects: (i) The phase boundary of olivine is generally formed parallel to the *a*-axis.[21,36,37] (ii) Orientations of phase boundaries depend on the degree of coherency. (iii) The largest lattice misfit was observed for *a*-axis. *b* and *c*-axis show relatively small lattice misfit as shown in supporting Figure 2s and Figure 3s. In Figure 6, we plotted the calculated *a* lattice misfit from Vegard's law $(a_{Li\text{-}rich} - a_{Li\text{-}poor})/a_{Li\text{-}rich}$ of $xLiFePO_4$, $yLiMnPO_4$ and $zLiCoPO_4$ ($x + y + z = 1$) for $LiFe_xMn_yCo_zPO_4$. Interestingly, we can confirm that higher than ~5.1% *a* lattice misfit induces two-phase reaction in the multi-component olivine, while less than ~5.1% shows full one-phase reaction during charging/discharging. This observation implies that general alloy theory can also be applied to the phase behaviors in the olivine materials. While the coherency strain from less than critical lattice misfit generally suppresses phase segregation, two-phase behavior is induced with the misfit larger then critical value because the coherency is too large to be stored in the crystal structure.

It should be noted that the misfit close to the critical value, even though it is smaller, can induce some degree of broken bond, dislocation or incoherency in the crystal structure.[21,38] Also, before concluding, it is worth to mention that there is a possibility that the observed peak broadening of XRD may have been derived from the presence of multiple single-phase particles with slightly different Li compositions ($0.5 - \delta \leq x \leq 0.5 + \delta$) similar to "mosaic" model,[39,40] while further study needs to be carried out to clarify.

Conclusions

The phase behavior of multi-component olivines was investigated by analyzing the structural evolution of a series of $LiFe_xMn_yCo_{1-x-y}PO_4$ ($0 < x, y < 1$) upon delithiation. While the one-phase reaction that was generally observed in multi-component olivines upon de/lithiation could be understood with the enthalpy of mixing presumably dominated from the electrostatic interaction among cations, strong two-phase behavior was observed as Mn substitution increased. A the higher Mn contents, with lattice misfit higher than ~5.1%, the multi-component olivines were prone to phase separate, whose critical misfit value is well corresponded with the general alloy theory. The preference for a two-phase reaction vs. a one-phase reaction in the olivine is believed to be the result of two competing factors: effective electrostatic between cations in the framework and

the degree of lattice misfit. Since electrochemical performance metrics such as rate capability and voltages are critically dependent on the structural evolution of the electrode upon cycling, we believe that investigating phase behavior of multi-component olivine materials will provide the insight needed to further improve the electrochemical performance of the olivine cathode for rechargeable lithium batteries.

Acknowledgments

This work was supported by a grant from the Fundamental R&D Program for Technology of World Premier Materials funded by the Ministry of Knowledge Economy, Republic of Korea and by Human Resources Development of the Korea Institute of Energy Technology Evaluation and Planning (KETEP) grant funded by the Korea government Ministry of Knowledge Economy (20114010203120). This work was also supported by Energy Efficiency and Resources R&D program (20112020100070) under the Ministry of Knowledge Economy, Republic of Korea. This work was also supported by the Industrial Strategic Technology Development Program (No.10038617, Development of Next Generation Lithium Metal Battery for the Full EVs) funded by the Ministry of Knowledge Economy (MKE, KOREA). This work was also supported by the National Research Foundation of Korea Grant funded by the Korean Government (MEST) (NRF-2009-0094219).

Supporting Information Available.— SEM images, ICP test results and Lattice parameter of synthesized samples.

References

1. A. K. Padhi, K. S. Nanjundaswamy, and J. B. Goodenough, *J. Electrochem. Soc.*, **144**, 1188 (1997).
2. G. Y. Chen, X. Y. Song, and T. J. Richardson, *Electrochemical and Solid State Lett.*, **9**, A295 (2006).
3. F. Zhou, T. Maxisch, and G. Ceder, *Phys. Rev. Lett.*, **97**, 155704 (2006).
4. C. Delmas, M. Maccario, L. Croguennec, F. Le Cras, and F. Weill, *Nat. Mater.*, **7**, 665 (2008).
5. L. Laffont, C. Delacourt, P. Gibot, M. Y. Wu, P. Kooyman, C. Masquelier, and J. M. Tarascon, *Chem. Mater.*, **18**, 5520 (2006).
6. C. Delacourt, P. Poizot, M. Morcrette, J. M. Tarascon, and C. Masquelier, *Chem. Mater.*, **16**, 93 (2004).
7. H. Huang, S. C. Yin, and L. F. Nazar, *Electrochemical and Solid State Lett.*, **4**, A170 (2001).
8. P. S. Herle, B. Ellis, N. Coombs, and L. F. Nazar, *Nat. Mater.*, **3**, 147 (2004).
9. F. Zhou, M. Cococcioni, K. Kang, and G. Ceder, *Electrochem. Commun.*, **6**, 1144 (2004).
10. S. Y. Chung, J. T. Bloking, and Y. M. Chiang, *Nat. Mater.*, **1**, 123 (2002).
11. A. Yamada, Y. Takei, H. Koizumi, N. Sonoyama, R. Kanno, K. Itoh, M. Yonemura, and T. Kamiyama, *Chem. Mater.*, **18**, 804 (2006).
12. D.-H. Seo, G. Gwon, S.-W Kim, J. Kim, and K. Kang, *Chem. Mater.*, **22**, 518 (2009).
13. K. S. Kang, Y. S. Meng, J. Breger, C. P. Grey, and G. Ceder, *Science*, **311**, 977 (2006).
14. S. Nishimura, G. Kobayashi, K. Ohoyama, R. Kanno, M. Yashima, and A. Yamada, *Nat. Mater.*, **7**, 707 (2008).
15. P. Gibot, M. Casas-Cabanas, L. Laffont, S. Levasseur, P. Carlach, S. Hamelet, J. M. Tarascon, and C. Masquelier, *Nat. Mater.*, **7**, 741 (2008).
16. S.-W. Kim, T. H. Han, J. Kim, H. Gwon, H.-S. Moon, S.-W. Kang, S. O. Kim, and K. Kang, *ACS Nano*, **3**, 1085 (2009).
17. C. Delacourt, P. Poizot, J.-M. Tarascon, and C. Masquelier, *Nat. Mater.*, **4**, 254 (2005).
18. H. Gwon, D.-H. Seo, S.-W. Kim, J. Kim, and K. Kang, *Adv. Funct. Mater.*, **19**, 3285 (2009).
19. A. Yamada, Y. Kudo, and K. Y. Liu, *J. Electrochem. Soc.*, **148**, A1153 (2001).
20. M. Wagemaker, D. P. Singh, W. J. H. Borghols, U. Lafont, L. Haverkate, V. K. Peterson, and F. M. Mulder, *J. Am. Chem. Soc.*, **133**, 10222 (2011).
21. D. A. Cogswell and M. Z. Bazant, *ACS nano*, **6**, 2215 (2012).
22. F. Zhou, C. A. Marianetti, M. Cococcioni, D. Morgan, and G. Ceder, *Phys. Rev. B*, **69**, 201101 (2004).
23. Y.-U Park, J. Kim, H. Gwon, D.-H Seo, S.-W Kim, and K. Kang, *Chem. Mater.*, **22**, 2573 (2010).
24. R. Shannon, *Acta Crystallographica Sec., A*, **32**, 751 (1976).
25. P. Bai, D. A Cogswell, and M. Z. Barant, *Nano letters*, **11**, 4890 (2011).
26. R. Malik, F. Zhou, and G. Ceder, *Phys. Rev. B*, **79**, 214201 (2009).
27. A. Yamada, Y. Kudo, and K. Y. Liu, *J. Electrochem. Soc.*, **148**, A747 (2001).
28. B. D. Cullity and S. R. Stock, *Elements of X-ray diffraction*, p. 176, Prentice Hall, New jersey (2001).
29. A. Yamada, M. Hosoya, S.-C. Chung, Y. Kudo, K. Hinokuma, K.-Y. Liu, and Y. Nishi, *J. of Power Sources*, **119**, 232 (2003).
30. C. A. Marianetti, D. Morgan, and G. Ceder, *Phys. Rev. B*, **63**, 224304 (2001).
31. D. A. Porter and K. E. Easterling, *Phase transformation in metals and alloys*, p. 157, Chapman & Hall, London, (1992).
32. M. Tang, W. C. Carter, and Y.-M Chiang, *Annu. Rev. Mater. Res.*, **40**, 501 (2010).
33. A. Van der ven, K. Garikipati, S. Kim, and M. Wagemaker, *J. Electrochem. Soc.*, **156**, A949 (2009).
34. A. G. Khachaturyan, *Phys. Stat. Sol.*, **35**, 119 (1969).
35. J. W. Cahn, *Acta Metall.*, **9**, 795 (1961).
36. G. K. Singh, G. Ceder, and M. Z. Barzant, *Electrochim. Acta*, **35**, 7599 (2008).
37. M. Tang, J. F. Belak, and M. R. Dorr, *J. Phy. Chem. C*, **115**, 4922 (2011).
38. L. Laffont, C. Delacourt, P. Gibot, M. Y. Wu, P. Kooyman, C. Masquelier, and C. Tarascon, *Chem. Mater.*, **18**, 5520 (2006).
39. W. Dreyer, J. Jamnik, C. Guhlke, R. Huth, J. Moskon, and M. Gaberscek, *Nature Mater.*, **9**, 448 (2010).
40. T. Ferguson and M. Bazant, *J. Electrochem. Soc.*, **12**, A1967 (2012).
41. See supplementray materials at http://dx.doi.org/10.1149/2.036303jes.